sustainability

MDPI

Article

Research on Deformation and Failure Law of the Gob-Side Roadway in Close Extra-Thick Coal Seams

Shengquan He [1,2], Le Gao [1], Bin Zhao [3,4,*], Xueqiu He [1], Zhenlei Li [1], Dazhao Song [1], Tuo Chen [5], Yanran Ma [1] and Feng Shen [1]

1 Key Laboratory of Ministry of Education for Efficient Mining and Safety of Metal Mine, University of Science & Technology Beijing, Beijing 100083, China
2 State Key Laboratory of Coal Mining and Clean Utilization, Beijing 100013, China
3 School of Safety Engineering, China University of Mining and Technology, Xuzhou 221116, China
4 China Coal Datong Energy Co., Ltd., Datong 037038, China
5 Department of Mining and Materials Engineering, McGill University, Montreal, QC H3A 0E8, Canada
* Correspondence: zhaobin_tashan@163.com

Abstract: To reveal the deformation and failure law of the gob-side roadway (GSR) and the main influencing factors in close extra-thick coal seams, the research methods of field monitoring, theoretical analysis, and numerical simulation are adopted in this paper. Field monitoring data shows that microseismic events occur and accumulate frequently in the surrounding rock and some overlying key layers of the GSR. Large deformation is experienced in the middle part of roadway near the solid coal side, the middle and upper parts of the roadway near the coal pillar side, and the roadway floor. The overlying strata of the GSR are fractured to form a composite structure as "low-level cantilever beam and high-level masonry beam". The coal pillar is squeezed and effected by the composite beam structure and the rotation moment M, causing serious bulge in middle and upper part of the coal pillar side. The stability of the solid coal side of the roadway is affected by the stress transferred from gangue contact point. Numerical simulation shows that the immediate roof and key layer breakage are induced by the mining of the 30,501 working face. Shear and tension failures happen in the GSR due to overburden subsidence and rotary extrusion. The stress and displacement at the middle and upper of the roadway on the coal pillar side are larger than the other area. Compared with the solid coal side, the coal on the coal pillar side is obviously more fractured, with a lower bearing capacity. The peak stress in the coal pillar shows up 2 m away from the roadway, which is close to the length of bolt support. The mining-induced stress and the stress transferred from gangue contact point are the direct reasons for solid coal bulge beside the roadway. The peak stress on the solid coal side is located 7 m away from the roadway, at the gangue contact point where overburden fractures. The overburden strata loads and the transferred stress near the gangue contact point are transferred from the sides to the roadway floor. Their coupling effect with the in situ horizontal stress acts as the force source for the plastic floor heave.

Keywords: near coal seams; gob-side roadway; microseismicity; overburden fracture; roadway deformation

check for updates

Citation: He, S.; Gao, L.; Zhao, B.; He, X.; Li, Z.; Song, D.; Chen, T.; Ma, Y.; Shen, F. Research on Deformation and Failure Law of the Gob-Side Roadway in Close Extra-Thick Coal Seams. *Sustainability* **2023**, *15*, 2710. https://doi.org/10.3390/su15032710

Academic Editor: Jianjun Ma

Received: 20 December 2022
Revised: 31 January 2023
Accepted: 31 January 2023
Published: 2 February 2023

Copyright: © 2023 by the authors. Licensee MDPI, Basel, Switzerland. This article is an open access article distributed under the terms and conditions of the Creative Commons Attribution (CC BY) license (https://creativecommons.org/licenses/by/4.0/).

1. Introduction

With the increasing demands of coal resources and the construction of resource-saving coal mines, the implementation of narrow coal pillars to arrange working faces has become a more popular choice of more mines [1–3]. However, large deformation and damage of the GSR has also become a large problem, plaguing safe production in mines, especially for close extra-thick coal seams.

Researchers have carried out a lot of research on the deformation and damage laws of GSRs and achieved fruitful results. Yang et al. [4] studied the bearing capacity of narrow coal pillars in the GSR during the process of mining by combining SMP criterion and numerical simulation. Wang et al. [5] studied the fracturing law of overburden during the process of multi-coal mining to determine the relationship between overburden structure failure and GSR deformation using UDEC simulation. Xu et al. [6] analyzed the damage characteristics of the GSR during fully-mechanized caving mining. They concluded that the non-uniform stress distribution during mining is the direct reason for the asymmetric roadway deformation and damage. Liu et al. [7] analyzed the failure mechanism and control technology of the GSR retaining in a short-distance coal seam. The damage and separation of the roof are the main causes of roadway instability. He et al. [8] researched the surrounding rock deformation mechanism during reuse of the gob side entry, and concluded that the surrounding rock failure is mainly affected by the advance abutment pressure. Shi et al. [9] researched the stability of surrounding rock in GSR driving in a deep and thick seam and concluded that the displacement and plastic zone of the surrounding rock of the straight wall semi-circular arch roadway are smaller than the corresponding deformation value of the surrounding rock of the rectangular roadway. Xiong et al. [10] put forward a concept of cyclic damage of the GSR in inclined coal seams, which was verified using numerical simulation. Wang et al. [11], Ma et al. [12], and Gao et al. [13] simulated the stress field, displacement, and plastic zone distribution of rock surrounding roadway when mining coal pillars with different widths. Wang et al. [14] analyzed the relationship between GSR damage and the basic roof fracturing location. They proposed that the roadway stability has a direct relationship with the breaking location of the key block. Additionally, the breaking laws of key blocks were analyzed with the roadway arranged at different positions during the face mining. Mo et al. [15] considered that the strength difference of the surrounding rock would impact the roadway and proposed that the displacement and failure mode of the surrounding rock were sensitive to deformation modulus. Li et al. [16] studied the relationship of in situ stress with roadway deformation and failure and proposed that the roadway layout should be parallel to the maximum horizontal stress. They believed that the concentrated stress at the top corner of the working face should be reduced in advance and the coal seam should be reinforced immediately after excavation. Zhao et al. [17] established a mechanical model of overburden strata on the GSR at the full-mechanized caving face in extra-thick coal seams. The mechanical source of the asymmetric failure of the GSR roof was obtained. Hua et al. [18] reported the mechanical connection between the roadway roof and the gob side roof and obtained the roadway stability mechanism and main roof stability criterion under the dynamic static coupling effect. Zhang et al. [19] studied the deformation and failure law of the GSR in deep mining condition and determined that the face mining and the coal damage are the direct causes of roadway deformation and damage. Guo et al. [20] studied the deformation characteristic of surrounding rock in GSR retaining formed automatically, and determined that the length of roof suspension is the main factor for stress distribution and deformation of the surrounding rock. Zha et al. [21] analyzed the deformation and failure characteristics of the rock surrounding the GSR with narrow coal pillars. The reasonable coal pillar size and roadway excavation time after mining were obtained. They also put forward surrounding rock control technology and effective roadway-side sealing technology. Zhou et al. [22] aimed at the stability of the floor, established a mechanical model to analyze the stability of the roadway floor heave by analogy with the basement heave of the deep foundation pit. It provides a model reference for analyzing the problem of roadway floor heave. Li et al. [23] researched the distribution of in situ stress in a deep roadway by adopting the combination of the stress measurement and comprehensive experimental research method and concluded that the horizontal stress is the key factor for determining the failure depth of the floor. Li et al. [24], Liu et al. [25], Zhang et al. [26], and Xue et al. [27] pointed out that the high stress, low bearing capacity of surrounding rocks and the existing support system are not effective to restrain the rock weathering, which are direct reasons for strength weakening in the deep roadway during the mining process. They proposed that using grouting and high-strength anchor support is an effective measure to ensure roadway stability.

To sum up, our predecessors carried out a lot of research on the deformation and damage laws of GSRs. However, the deformation and failure laws of GSRs and the main influencing factors in close extra-thick coal seams are not clearly revealed.

In this study, a typical GSR of the 30,503 working face in Tashan Coal Mine was investigated to determine deformation and failure characteristics of the GSR via field measurement, theoretical analysis, as well as numerical simulation. The structural characteristics of overburden and its influence on the stress and displacement fields of surrounding rock are obtained. The deformation and failure laws of the GSR and the main influencing factors are revealed. The research results could lay a theoretical foundation for the stability control of the GSR in similar mining conditions.

2. Engineering Background and Roadway Deformation Characteristics

2.1. Temporal and Spatial Evolution Laws of Microseismic Events

#3–5 coal seam of Tashan Coal Mine is extra-thick coal seam, with an average burial depth of 435 m. The Coal Mine is located in Yungang District, Datong City, Shanxi Province, China. The mine field area is 8.146 km^2. The layout of the working face and roadway is shown in Figure 1 (for more details about engineering background please refer to Zhao et al. 2022 [28]). The 30,503 working face passed through the filled roadway on 19 January 2021. To determine the damage characteristics of the GSR before and when the working face passed through the filled roadway, the microseismic monitoring data during these periods were analyzed. The temporal-spatial distribution law of microseismic events near the GSR are shown in Figures 2 and 3. Orlecka-Sikor reported that the concentration area of microseismic events is mainly the stress concentration area [29]. It can be seen from the plan distribution of microseismic events in Figure 2 that the frequency and energy of microseismic events increase significantly as the working face is near the filled roadway, and they are more concentrated near the GSR. This indicates that mining towards the filled roadway area led to the increasing of stress concentration and damage on the gob side. The sectional distribution of microseismic events is shown in Figure 3; the events increase significantly and their range expands along the strike obviously as the work faces get closer to filled roadway, indicating higher mining-induced stress when the working face passed through the filled roadway.

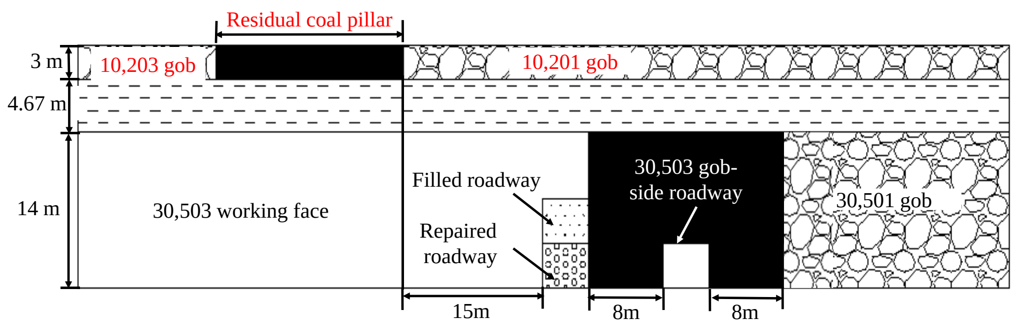

Figure 1. Layout of the 30,503 working face [28].

The overlying microseismic events of the GSR are mainly concentrated in the range 100 m above the coal seam floor. The key layer with thickness of 51 m has frequent fracturing events. The accumulation and frequency of microseismic events in the surrounding GSR, roof, and floor of the adjacent roadway indicate that the area is in a high stress concentration area, which could be the direct cause of large deformation of the roadway.

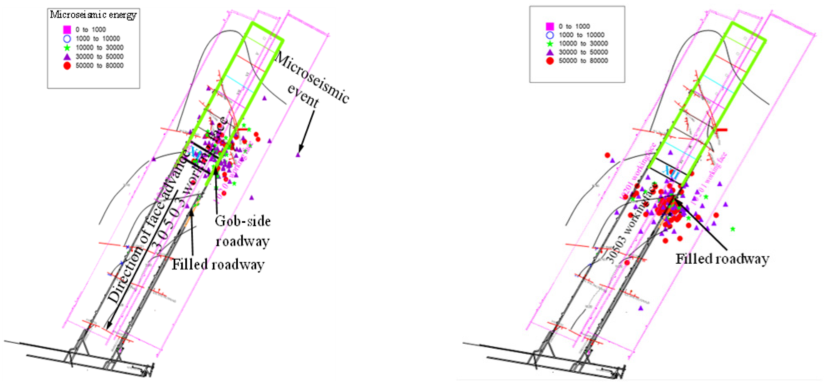

(**a**) November 2020 (**b**) December 2020 (**c**) January 2021

Figure 2. Microseismic events distribution before and during the working face passes through the filled roadway.

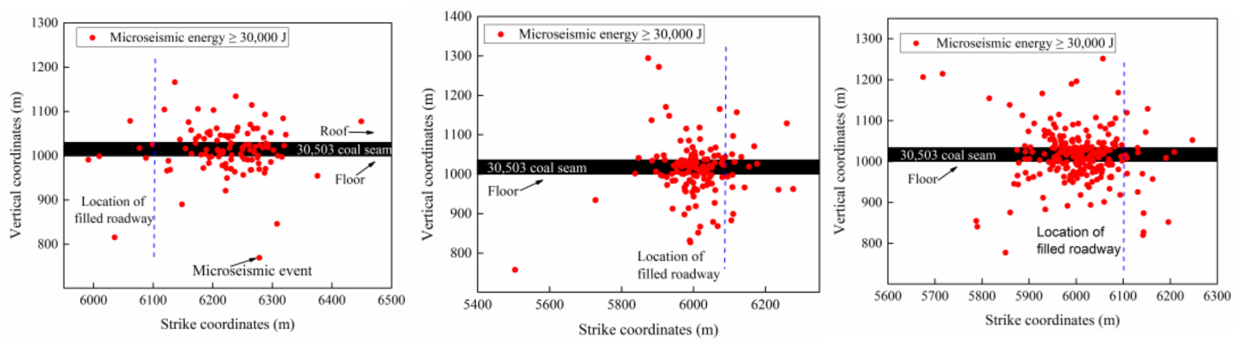

(**a**) November 2020 (**b**) December 2020 (**c**) January 2021

Figure 3. Microseismic events distribution before and during the working face passes through the filled roadway. Blue dotted line is the location of filled roadway.

2.2. Deformation and Damage Characteristics of the Roadway

As shown in Figure 4, the on-site observation shows that the 30,503 working face of the GSR is severely affected by mining. The deformation of the middle part of the solid coal side, the middle and upper part of the coal pillar side, and the bottom of the roadway are considerably large. During mining the 30,503 working face, the GSR received relatively serious deformation and damage. Floor heave begins to appear on the floor within 200 m in front of the working face, reaching 0.5–0.7 m relevant height, causing the concrete laid on the floor to crack. After the roadway floor is repaired, the amount of heave on the floor continuously increases as the working face gets closer. Both sides of the roadway have serious bulge, and the deformation for the middle and upper part of the coal pillar side is more dramatic compared with the solid coal roadside. Although the roadway is supported by bolts, the large pressure still causes the roadway sides to fracture, and embeds bolts and anchor cable trays in the coal seam.

The 30,503 working face of Tashan Coal Mine was mined to the filled road area on 19 January 2021. The deformation data of the two roadsides before and after the working face passes through the filled roadway were monitored to reveal the influence of the filled roadway on the deformation and damage of the GSR, and the results are shown in Figure 5. The maximum deformation of the two sides of GSR is 200 mm before the working face passes through the filled roadway, and the maximum deformation of the GSR is 660 mm when mining to the corresponding area of the filled roadway. It means that the existence of the filled roadway affects the stability of the GSR in the process of coal seam mining. The support strength should be increased in the area where the filled roadway exists.

(**a**) Coal pillar side bulge

(**b**) Solid coal side bulge

Figure 4. Deformation and damage characteristics of GSR.

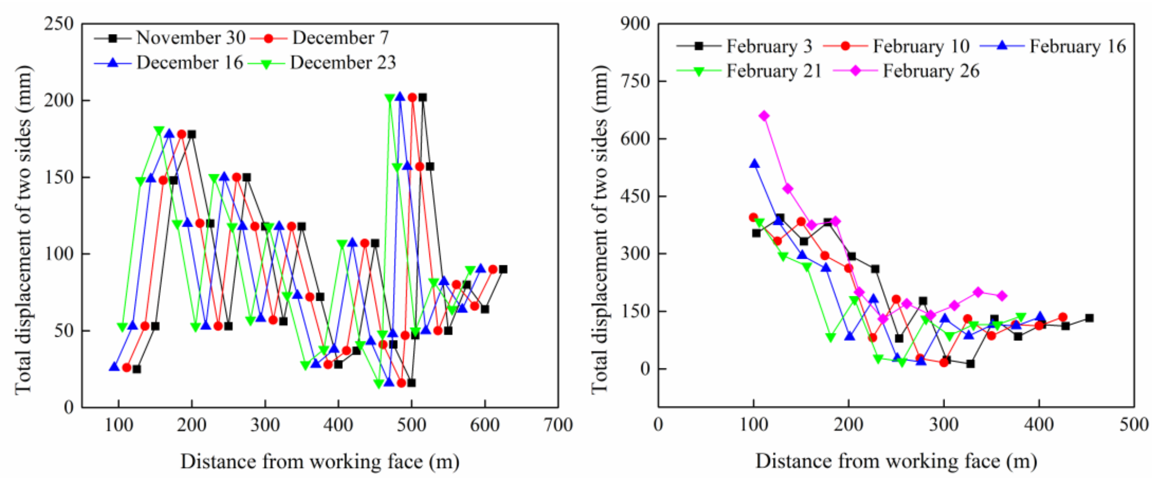

(**a**) Before mining to filled roadway (**b**) Mining to filled roadway

Figure 5. Displacement of two sides of the GSR at different monitoring days.

3. Mechanical Analysis of the Influence of Overburden Structure on the Roadway Stability

3.1. Fracturing Law of Overburden Structure of GSR under Repeated Mining

#3–5 coal seam of the Tashan Coal Mine is typical close extra-thick coal seams. Its distance to the gob of overlying #2 coal seam is only 4.6 m. Since the mining thickness of #3–5 coal seams in one step is 14 m, the gob is greatly increased compared with the #2 coal seam. Therefore, the structural stability of strata overlying the GSR under repeated mining needs to be explored.

There is a 7.9 m thick low-level old roof and a 51.2 m thick high-level old roof overlying the Tashan Coal Mine from borehole histograms. After the #2 coal seam was mined, the low-level old roof was fractured to form a masonry beam structure. After the 30,501 working face is mined, whether the low-level old roof can form a stable structure can be assessed by Formula (1). When the condition is met, the structure can be formed as a cantilever beam [30]:

$$\Delta > \Delta_{\max} \tag{1}$$

where Δ is the rotation amount after the rock strata is broken, $\Delta_{\max}$ is the limit rotation required for the breaking block of the key layer to be hinged to form a stable "masonry beam" structure.

$$\Delta = M_1(1-\mu) - \sum h_i(K_p - 1) > \Delta_{\max} = h - \frac{ql^2}{kh\sigma_c} \tag{2}$$

where $\sum h_i$ is immediate roof thickness, K_p is rock fragmentation expansion coefficient, h is the thickness of broken rock stratum, k is dimensionless coefficient, l is periodic step distance of rocks, σ_c is compressive strength of rock, μ is coal caving loss rate, M_1 is coal seam thickness, q is overburden load, $q = \lambda H$, λ is unit weight of rock, H is burial depth of rock.

According to the measured data of Tashan Coal Mine, M_1 is 14 m, $\sum h_i$ is 18.19 m, K_p is 1.2, μ is 15%, the periodic step distance of the low-lever old roof is measured to be 19.8 m, q is 10,625 KN/m^3 and σ_c is 76 MPa. The above parameters are substituted to Formula (1), Δ = 6.44 m, $\Delta_{\max}$ = 5.33 m. It shows $\Delta > \Delta_{\max}$ to satisfy Formula (1). Therefore, the low-level old roof is broken to form a cantilever beam structure when the #3–5 coal seams are mined. The same theoretical calculation is used to get the rotation amount of the high-level old roof is 2.3 m, which is less than the maximum rotation amount of 3.6 m, forming a hinged masonry beam structure. From this, when the #2 coal seam and the 30,501 working face are mined, the overlying strata of the 30,503 GSR will form a "low-level cantilever beam and high-level masonry beam".

The breaking law of overlying rocks when the #2 and #3–5 coal seams are mined separately is analyzed to further determine the fracture law of the overlying high and low old roofs in the GSR under the influence of repeated mining. Firstly, the limit equilibrium theory is used to calculate the distance X_0 between the broken position of the low-level old roof and the coal wall of the working face, when the #2 coal seam is mined [31]:

$$X_0 = \frac{M_2 A}{2\tan\varphi_0} \ln\left[\frac{K\gamma H' + C_0/\tan\varphi_0}{C_0/\tan\varphi_0 + P_0/A}\right] \tag{3}$$

where, M_2 is coal seam mining height, γ is unit weight, A is coefficient of lateral pressure, φ_0 is internal friction angle, K is stress concentration coefficient, C_0 is cohesion, H' is mining depth. P_0 is the support resistance of the support on the upper section level roadway to the lower side.

Combined with the field measured data and Formula (3), it is calculated that the breaking position of the low-level old roof after mining the #2 coal seam is 4.6 m away from the coal wall of the 10,201 gob. The corresponding position of gangue contact point after the breaking of the key block B on the low-level old roof is 15.2 m away from the remaining coal pillars, 26.8 m horizontally away from the 30,501 gob, and 13.8–18.8 m away from the 30,503 GSR. The remaining coal pillar is 28 m away from the narrow coal pillar of the GSR. The broken length of the low old roof is 19.8 m. When the key block of the low old roof fails, the failure position between block C and the adjacent block is 7 m away from the 30,501 gob, located 1 m above the narrow coal pillar with width 8 m and close to the roadway side. The remaining rock blocks with a distance of 12.8 m or shorter will form a cantilever beam structure. Because the narrow coal pillar is affected by the fracture position of the low cantilever beam, stress concentration can be formed on the coal pillar, which will lead to greater damage to the coal pillar. The schematic diagram of the broken structure of the low-level old roof is shown in Figure 6.

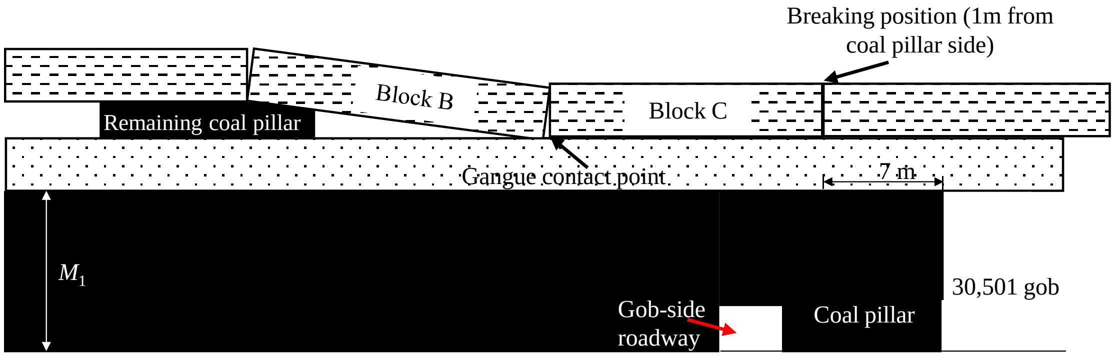

Figure 6. Sectional diagram of the rock layer overlying the GSR after the low-level old roof is broken.

The same calculation method is used to calculate that after mining the 30,501 working face, the periodic breaking length of the high-level old roof is 45.2 m, and the breaking position is 22 m away from the coal wall of the 30,501 gob. The corresponding position of the gangue contact point is 20 m away from the remaining coal pillar and 7–12 m away from the 30,503 GSR after the key block of the high-level old roof is broken. The distance between the breaking point of the high-level old roof and the gangue contact point on the low-level old roof is only 4.8m, according to theoretical calculation results. After the high-level rock beam breaks and sinks, part of the load acts on the gangue contact point, and the other part acts on the coal pillar, roof, and solid coal of the GSR. The load acting on the coal pillar will cause the roadway to deform. The stress around the gangue contact point will be concentrated and transferred to the #3–5 coal seams. The schematic diagram for the overlying rock layer of the GSR after the high-level old roof is broken is shown in Figure 7.

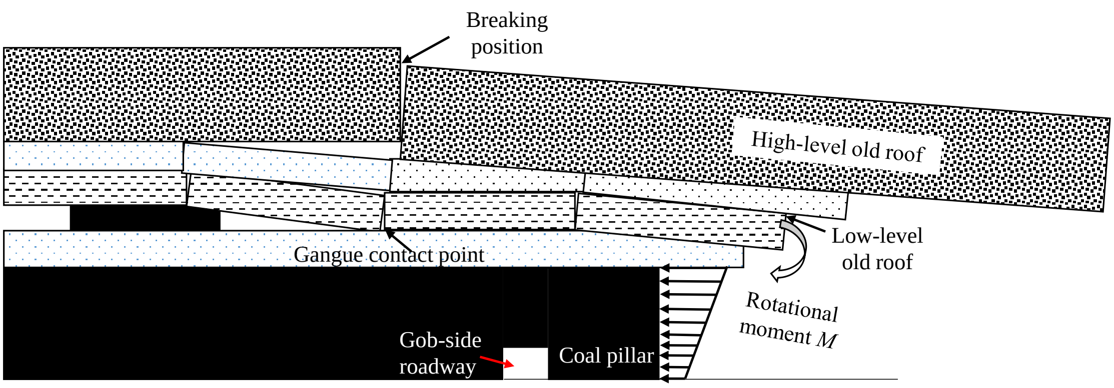

Figure 7. Schematic diagram of rock structure overlying GSR under repeated mining.

When the high-level old roof breaks and sinks on the lower cantilever beam, the cantilever beam will rotate under compressive stress and transfer a part of stress to the lower coal pillar. Combined with the research results of Qu et al. [32], when the high-level old roof breaks and sinks, the coal pillar is not only squeezed by overlying strata, but also is acted upon by the rotational moment M, as shown in Figure 7. The middle and upper part of the coal pillar are more obviously affected by the moment M, which is an important reason for the bulge of the middle and upper part of the coal pillar beside the GSR.

3.2. Stress Transfer Characteristics of Contact Gangue Point under the Action of Overburden Structure

According to the breaking law of overlying stratum of the GSR, the surrounding rock of the adjacent roadway is subject to the compressive stress of the high and low level old roof breaking on the coal body at the solid coal side and the high stress at the gangue contact point after the high and low level old roof breaking. The maximum transferred stress at the contact gangue point where the old roof is broken can be calculated by the following formula [32]:

$$\sigma_{\max} = \frac{\{\gamma(4H - 2L)[2L\tan\alpha + (H - L/2)\tan\alpha] + 2\gamma L^2 \tan\alpha}{4(a + h\cos\varphi\tan(\theta + \varphi) - h\sin\varphi)\tan^2\alpha} \quad (4)$$

where, a is the width of the coal pillar, h is the thickness of the middle layer between the #2 coal seam and the #3–5 coal seams, φ is the inclination angle of the coal seams, α is the gangue angle, L is the inclination length of the gob, and θ is the stress transferring angle.

The length of the stress transferring area at the gangue contact point is r. Taking the coal wall of the 30,501 gob on the right as the starting point, the stress transfer angle θ is shown in Figure 8. The transferred stress continues to increase from 0 on both sides of the contact gangue point and reach to the maximum value σ_{max} at the contact gangue point. The length r can be calculated through the model.

$$r = a + h\cos\varphi\tan(\theta + \varphi) - h\sin\varphi \quad (5)$$

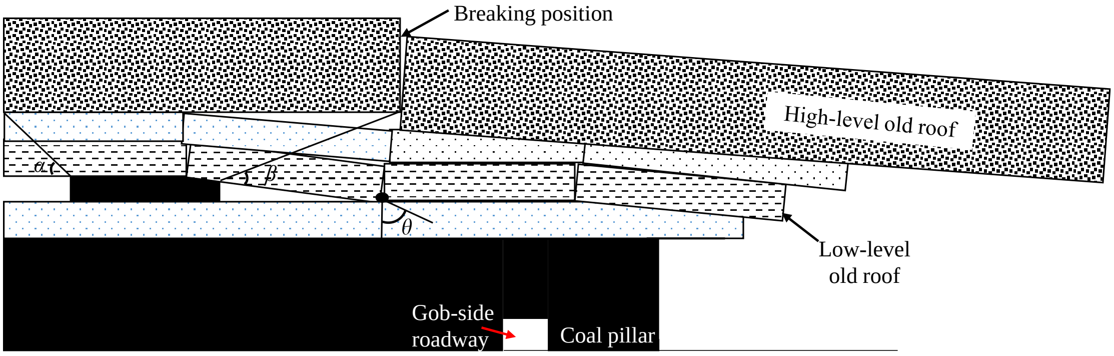

Figure 8. Sectional diagram of the stress transfer model at the contact gangue point.

According to the actual situation of the Tashan Coal Mine, the vertical distance between the #2 coal seam and the #3–5 coal seam is 4.6 m, the width of the narrow coal pillar is 8.0 m, θ is 30°, the dip angle of the coal seam φ is 2°. According to existing research results [32], the gangue angle α is 75° and the rock fracture angle β is 84°. The above data are substituted into Equations (4) and (5) to obtain σ_{max} at the contact gangue point is 23.74 MPa and r is 10.5 m. Combined with theoretical analysis, the breaking position of the old roof is 7–12 m away from the GSR, and the influence range of the contact gangue point stress is 10.5 m. Therefore, the transfer stress of the contact gangue point can affect the stability of the GSR after the high-level old roof breaks and touches the gangue.

Section 2.1 concluded that microseismic events occur frequently in the high and low-level old roof area above the GSR. The failure area of the high and low-level old roof obtained from the theoretical analysis is basically consistent with the microseismic event gathering area monitored on site, which verifies the accuracy of the theoretical analysis results. Simultaneously, the field monitoring shows that the upper and middle part of the coal pillar side of the roadway are seriously bulged compared to other areas, which further verifies the theoretical analysis that the composite structure of low-level cantilever beam and high-level masonry beam squeezed these areas. The stress transferring at the gangue contact point is the main reason for side wall bulge on the solid coal side in the field.

4. Numerical Simulation Research on Deformation and Damage Law of GSR in Close Extra-Thick Coal Seams

4.1. Model Construction and Research Plan

The numerical model is established in FLAC3D modelling software, taking the geological conditions of the Tashan Coal Mine as the engineering background, as shown in Figure 9. The model size is 640 m × 400 m × 130 m (XYZ), with 530,504 grids. The model uses hexahedral mesh. For more details about numerical model and boundary conditions, please refer to Zhao et al. 2022 [28].

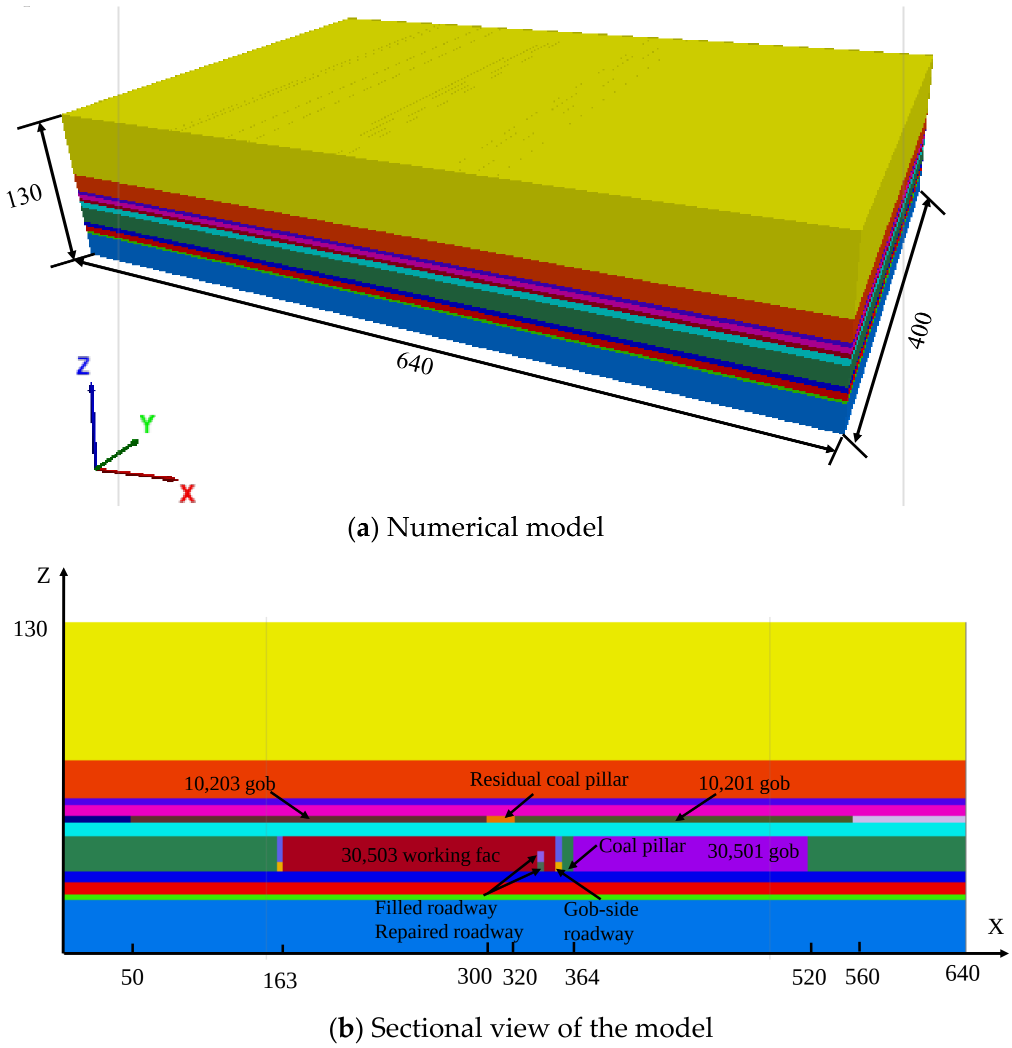

Figure 9. Numerical model.

The Mohr-Coulomb constitutive model [33] is used to reveal the deformation and damage law of the GSR in the close extra-thick coal seams. The physical and mechanical parameters used in the numerical model are from the experimental results of the coal and rock sample in the Tashan Mine [28].

To reflect actual mining conditions, the following mining sequence is simulated: (1) the 30,501 working face is mined with the historical mining sequence of the working face. The stress field and plastic zone of surrounding rock of the GSR of the 30,503 working face are analyzed before mining. (2) The impact of mining on the 30,503 working face stability is studied.

4.2. Distribution Laws of Stress Field and Plastic Zone Surrounding Roadway after GSR Excavation

Modelled excavation is carried out according to the actual mining sequence. The modelled roadway supports are consistent with the actual mine support method. The distribution laws of the stress field and plastic zone for rocks surrounding the GSR after GSR excavation are shown in Figures 10 and 11. As can be seen in Figure 10, the stress in the remaining coal pillar area of the overlying #2 coal seam is highly concentrated, and transferred the stress to the low-level coal mass and upper overlying stratums, with a maximum value of 47 MPa. The main reason for the stress concentration in the coal pillar area is that after the coal masses on the left and right sides of the coal pillar are mined, the overlying strata are in a suspended state, and the overlying stratum is mainly supported by the remaining coal pillars. It can be seen from Figure 11, under the compressive stress of overlying strata, the coal pillar undergoes obvious shear failure, which extends to the lower coal seams. The coal and rock mass near the GSR is affected by the overlying #2 coal seam. The mining of the right side of the 30,501 working face led to obvious pressure relief. Simultaneously, due to the mining of the 30,501 working face on the right side of the GSR, the 4.6 m-thick immediate roof collapsed and drove waste rocks from the mining settlement of the #2 coal seam to further collapse. Moreover, overlying sandstones with 51 m thick also fractured integrally to act on gob and narrow coal pillar. At this time, narrow coal pillars are the main support point of the overlying strata. Under the overlying rock subsidence and rotary extrusion, the stress in the narrow coal pillar area of the #3–5 coal seams increases with a maximum of 17 MPa in the junction area between the cantilever beam and the coal mass. The stress extends to the middle and upper area of the GSR. Shearing and tensioning damage occurred in the GSR due to the subsidence and rotary extrusion of overlying strata. The subsidence and extrusion of overlying key blocks on the coal pillar side is the main reason for the plastic failure of the side, as well as an important cause for the heave occurring in the middle and upper part of the coal pillar side, as obtained in Section 3.1. The vertical stress transmitted by the key blocks acts on the solid coal and coal pillars, which becomes a crucial cause of the floor heave. Based on the above analysis, it can be seen that after the adjacent working faces are mined, the squeezing effect after the key blocks above the GSR sank and broke is an important reason for the deformation and failure of the surrounding rock of the roadway.

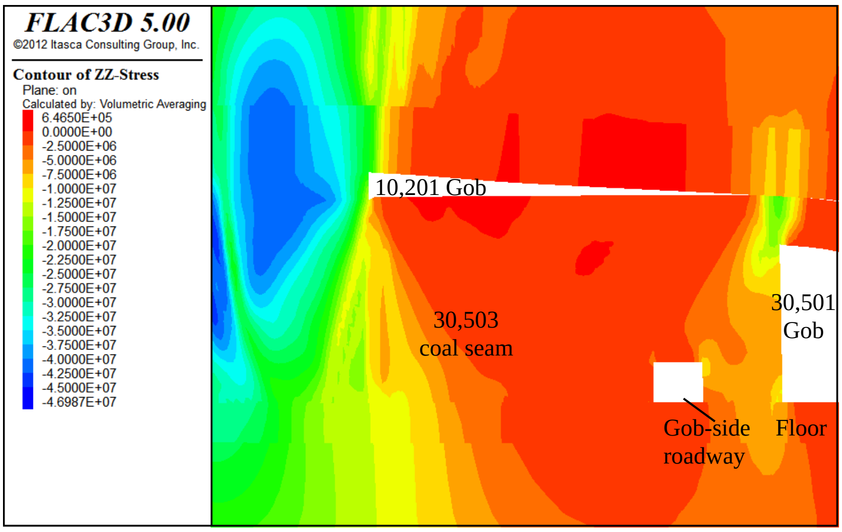

Figure 10. Stress contour of surrounding rocks after GSR excavation.

4.3. Influence Law of Mining Action on Stability of GSR in 30,503 Working Face

4.3.1. Variation Law of Advanced Support Pressure under the Influence of Mining

The field measurement shows that the advanced support pressure is one of the main reasons for the deformation and damage of the rock surrounding the GSR. Figure 12a shows the advanced support pressure distribution in the middle of the coal seams under different mining distances of the 30,503 working face. Figure 12a indicates that there are three stress peaks. The left and right peaks correspond to the stop mining line of overlying coal seam #2 and the open-off cut corresponds to the remaining coal body area, and the middle is the advanced support pressure peak area. When the 30,503 working face is mined 60 m, 80 m, 90 m, 100 m, and 110 m, respectively, the peaks of the advanced support pressure were 20 MP, 28 MPa, 31.2 MPa, 31 MPa, and 29 MPa, respectively. Stress peaks basically occur at the position 20 m ahead of the working face. When the working face is mined to 90–100 m, the advanced support pressure reaches the peak value, which means the working face has been fully mined. When mining to 100 m, the peak value in vertical stress distribution (Figure 12b) and the plastic zone distribution (Figure 12c) are also basically located at the position of 20 m ahead of the working face.

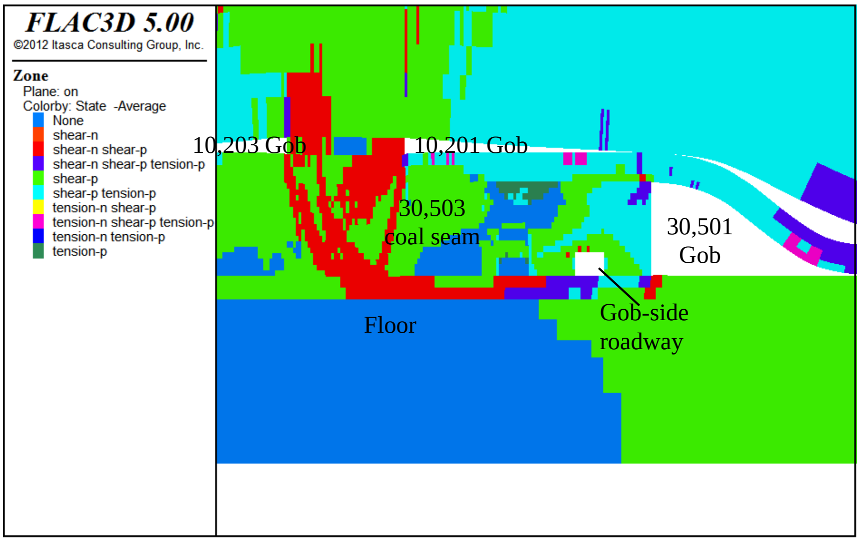

Figure 11. Distribution of plastic zone surrounding the GSR.

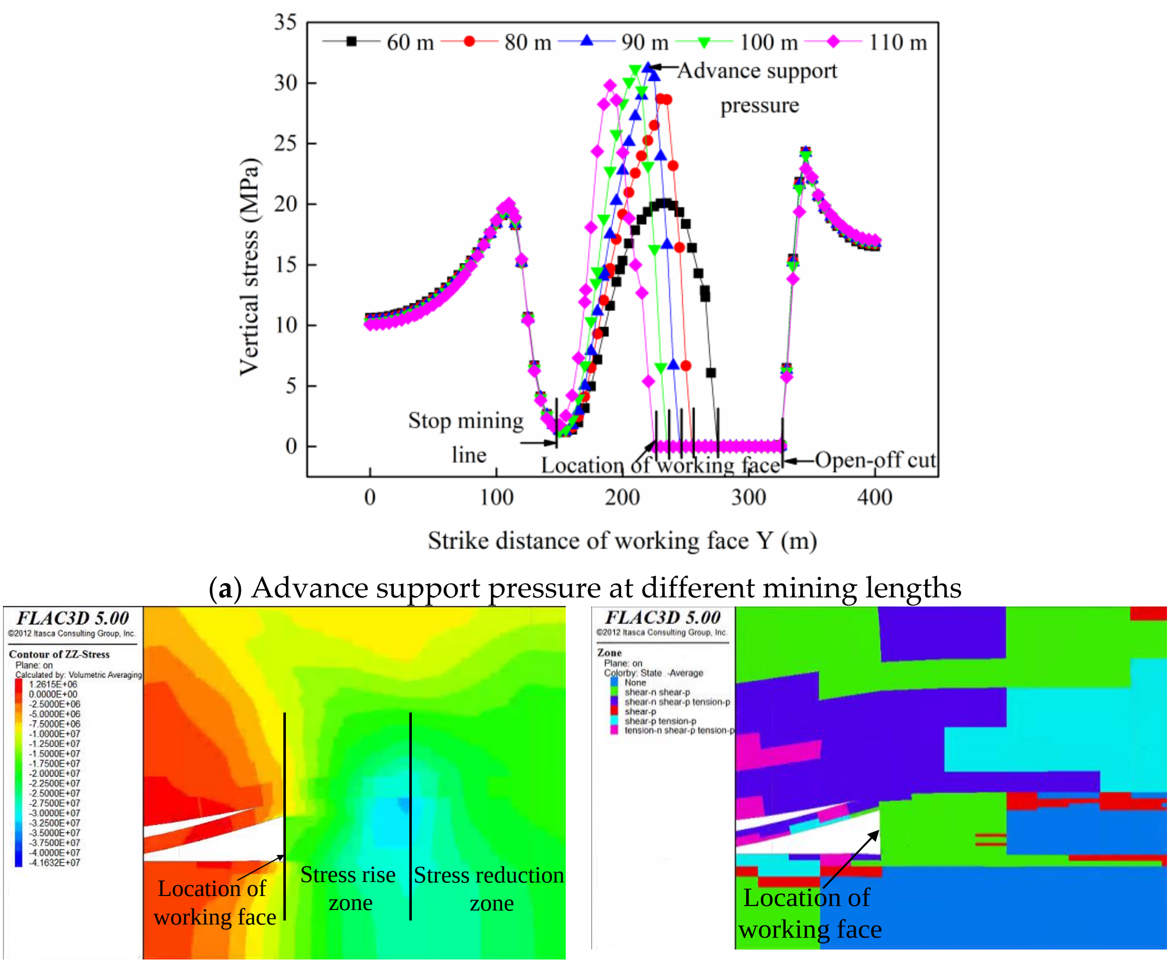

(**a**) Advance support pressure at different mining lengths

(**b**) Distribution of stress field (**c**) Distribution of plastic zone

Figure 12. Distribution of stress and plastic zone.

A total of six monitoring lines were arranged along the working face on the solid coal and coal pillar sides of the GSR, to further reveal the influence of mining the 30,503 working face on the surrounding rock stability of the GSR. The monitoring lines on the solid coal side are arranged 2 m away from the roadway with an interval of 2 m as lines 1, 2, and 3 sequentially from inside to outside. The coal pillar side is arranged similarly, as shown in Figure 13.

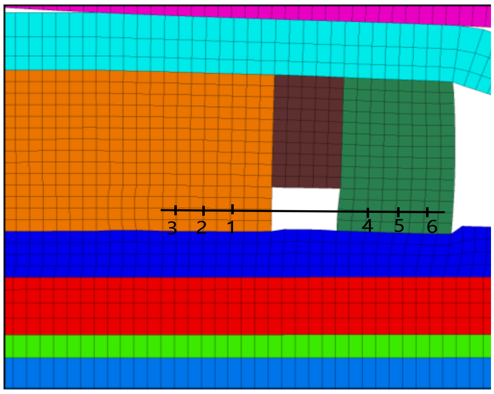

Figure 13. Layout of monitoring lines in two sides of the GSR. Different colors represent different coal and rock beds.

The vertical stress distribution of two roadway sides at different mining distances is simulated as shown in Figures 14–16:

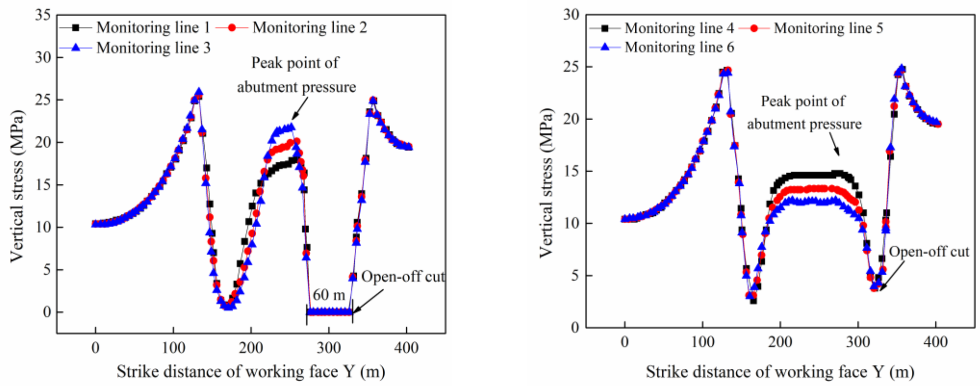

(**a**) Stress distribution on the solid coal side (**b**) Stress distribution on the coal pillar side

Figure 14. Vertical stress distribution when mining at 60 m.

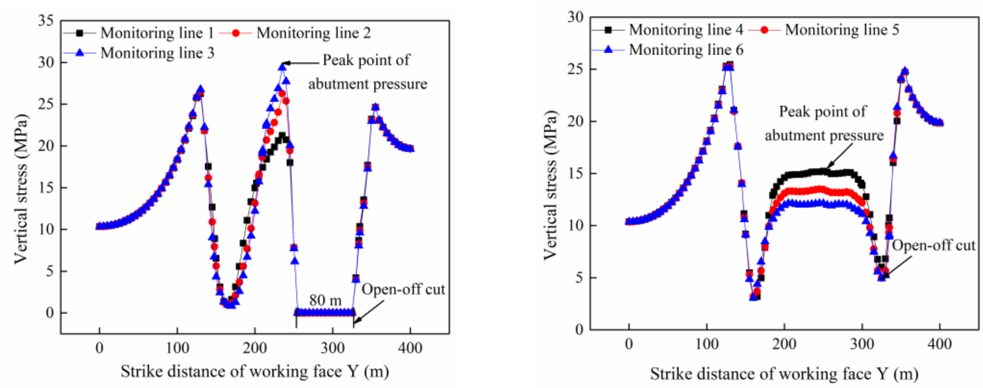

(**a**) Stress distribution on the solid coal side (**b**) Stress distribution on the coal pillar side

Figure 15. Vertical stress distribution when mining at 80 m.

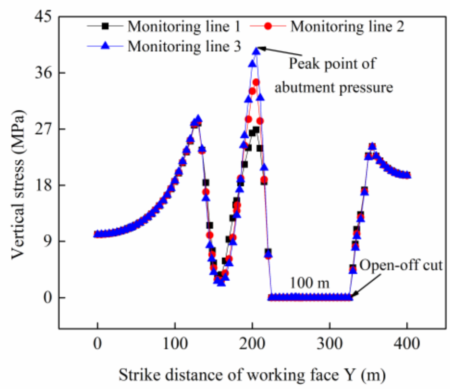

(**a**) Stress distribution on the solid coal side

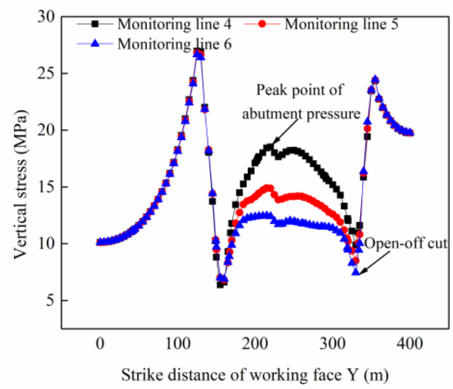

(**b**) Stress distribution on the coal pillar side

Figure 16. Vertical stress distribution when mining at 100 m.

The advance support pressure on the solid coal side of the roadway changes with the continuous advance of the mining face. When the working face is at 60 m, 80 m, and 100 m, respectively, the peak values of the advance support pressure are 21.6 MP, 29.3 MPa, and 39.1 MPa, respectively. With the advance of the working face, the stress peaks basically appear about 20 m in front of the working face, and the stress peaks also increase with the mining length. This is mainly due to the mining of the working face in the proximity of the 30,501 gob. Under the coupling action of the advanced bearing pressure and the lateral bearing pressure, the stress peak value increases continuously.

Comparing supporting pressures on the coal pillar side of the roadway under different mining distances, it can be seen that when the working face is at 60 and 80 m, the distribution trend of the supporting pressure is similar. The peak value of the bearing pressure on the coal pillar is stable at 12.1–15.2 MPa. However, when the working face is mined to 100 m, the peak support pressure is 18.5 MPa. The support pressure on the monitoring line 6 near the gob basically does not change, indicating that the coal in this area is very broken. The supporting pressures along the survey line 4 and line 5 have the increase of 2.77 MPa and 3.7 MPa, respectively, compared with that when the mining is at 80 m. This indicates that the compression effect from the overlying strata on the coal pillar near the gob is more dominant due to mining, which is in line with the theoretical analysis results.

The advanced support pressure variation in two sides of the roadway during mining shows that the peak value basically appears at about 20 m ahead of the working face. Also, the coal on the coal pillar side is significantly more broken than the solid coal side with lower carrying capacity. Within 8 m of the solid coal side, the coal body is more broken as it is closer to the roadway side and the coal pillar is more fragmented as it is closer to the gob. This is an important cause for roadway side walls bulging during mining.

4.3.2. Stress Distribution around the Roadway during Mining

Monitoring lines are arranged surrounding the roadway to further quantify the stress changes of the two sides and the floor of the roadway during mining. The length of the two-side monitoring lines is 8 m. Line A starts parallel to the roof. A total of eight lines are arranged with 1 m interval. Four 6 m long monitoring lines are arranged in the floor with an interval of 1 m. The layout of the monitoring lines is shown in Figure 17. The simulated working face is mined 100 m forward and the stress distribution law on the monitoring section at 0, 20, and 30 m ahead of the working face is extracted. The results are shown in Figure 18.

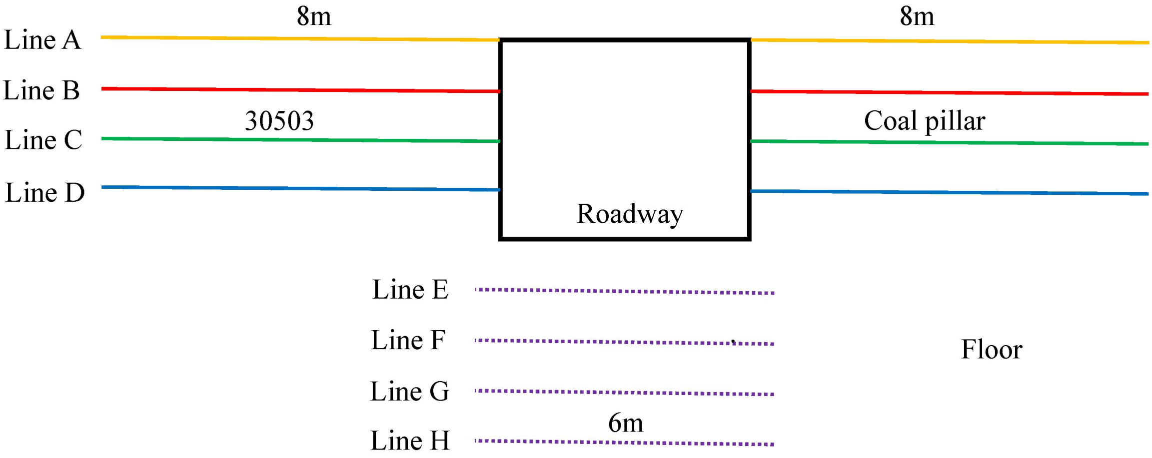

Figure 17. Sectional layout of the roadway monitoring lines.

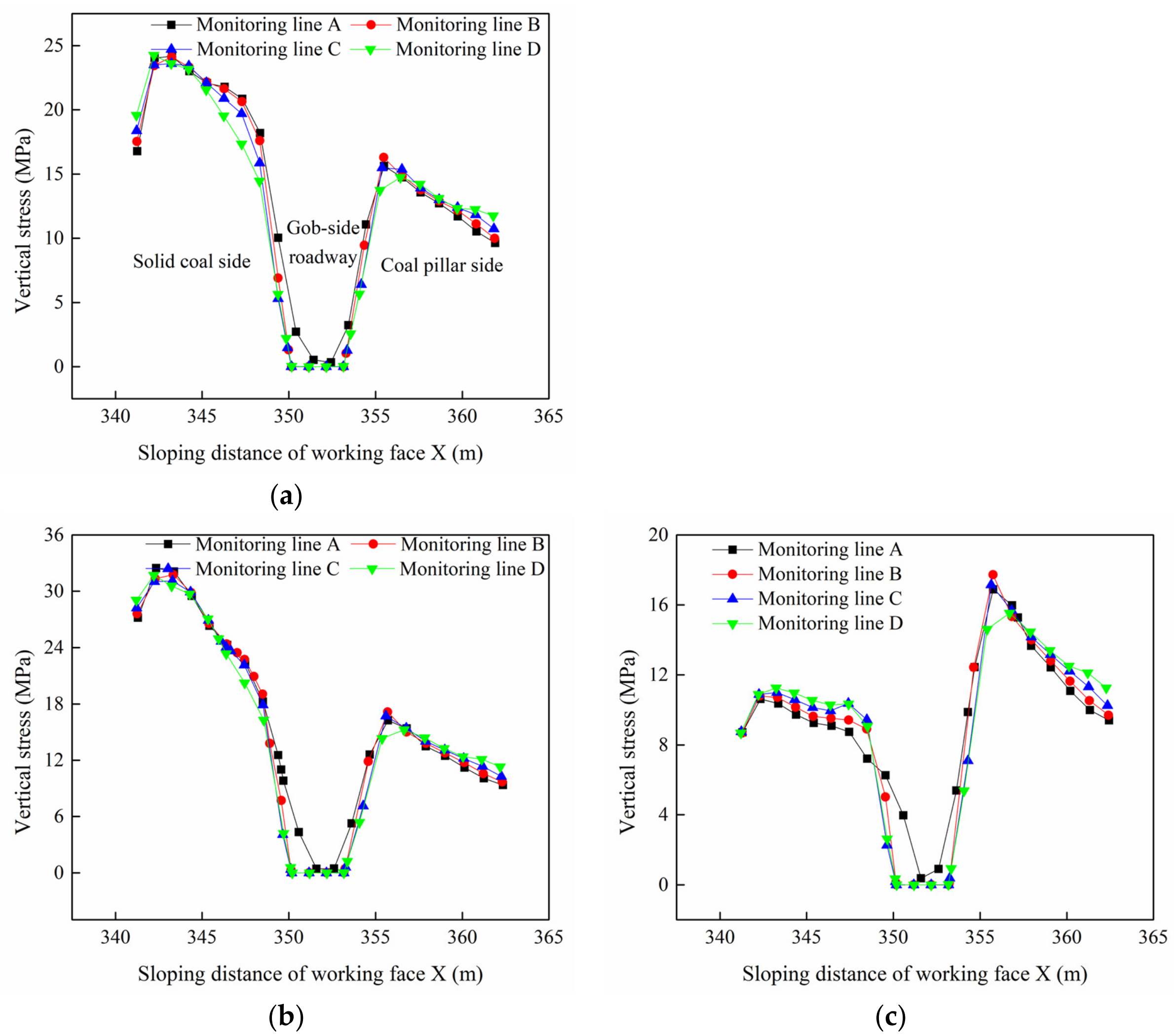

Figure 18. Monitored vertical stresses around the GSR. (**a**) 0 m ahead of the working face, (**b**) 20 m ahead of the working face, (**c**) 30 m ahead of the working face.

Figure 18 shows when the distance of mining to the working face is 100 m, the stress changing trend within 20 m ahead of the working face in solid coal side is basically the same, and its bearing capacity increases as it moves away from the roadway and its peak shows up at 7 m away from the roadway. The peak position is close to the theoretical calculation result in Section 3.1 located at the gangue contact point. The rise of the stress in solid coal side at an advance of 30 m is significantly lower than that within 20 m. It can be seen that the range of 20 m ahead of working face is the main mining affected area. Figure 18 shows that the peak stress on the coal pillar side within 30 m of the working face appears at 2 m near the roadway. 2.2 m bolts have been used for the two sides of roadway. The protection range is just in the peak stress range of the coal pillar side, which is an important reason for the damage and the bulge of bolts on the coal pillar side. The breaking position of the low-level old roof is 1 m away from the coal pillar, as calculated in Section 3.1. The numerical simulation is similar with the theoretical results. It can be seen from the stress distribution within 30 m, the peak stress in the roadway sidewall on the coal pillar side always appears at the position of monitoring lines A, B, and C. This stress distribution characteristic can explain the phenomenon for the heave and serious damage of the middle and upper coal pillar side onsite.

The stress of the solid coal side is significantly larger than that of the coal pillar side within 20 m ahead of the working face. The stress of the coal pillar side is larger at 30 m. This is because the coal pillar within the mining-influenced range is disturbed by repeated mining, yielding a reduced bearing capacity. The mining causes the high-level rock beam to break and in contact with the waste rock. In this case, the solid coal becomes the main bearing structure after the overlying key block is broken with a high stress concentration area appearing on the side. In the area not affected by mining, the coal pillar is relatively complete with the coal pillar as the main bearing structure after the overlying key block is broken. Thus, the stress increases under the compression of broken key block.

Figure 19 shows the monitoring results of the horizontal stress at each monitoring line in the two sides of the roadway. The measured horizontal stress of the solid coal at 20 m and 30 m ahead of the working face is greater than that on the coal pillar side of the roadway. The horizontal stress peaks appear at 2 m from the roadway on the coal pillar side and at 7 m on the solid coal side, which is consistent with the vertical stress peak position. The high horizontal stress on the solid coal side of the roadway is the direct cause for the heave on the solid coal side.

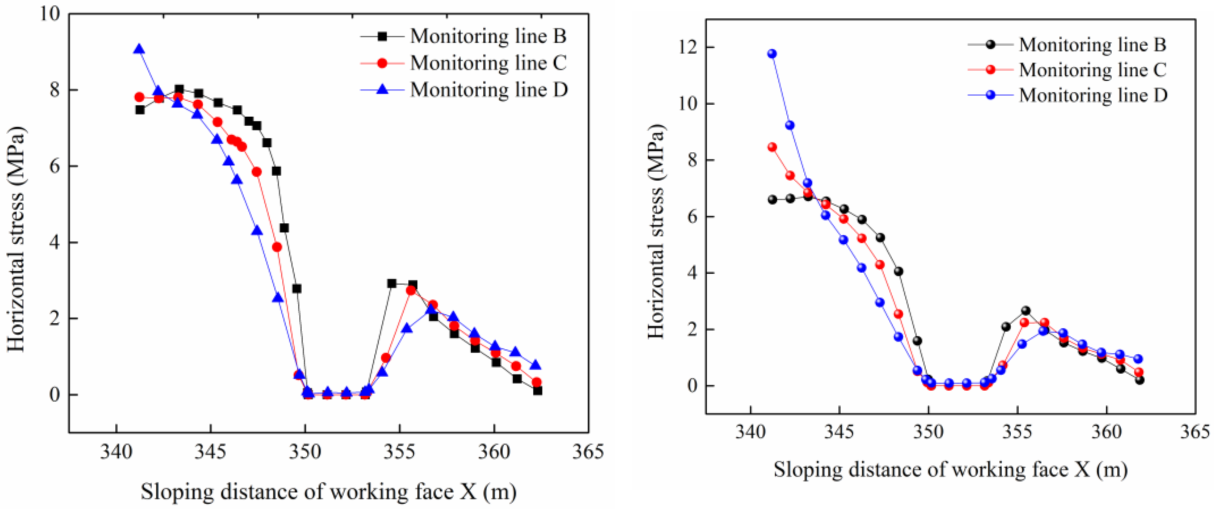

(**a**) 20 m ahead of the working face (**b**) 30 m ahead of the working face

Figure 19. Horizontal stress distribution of two sides of GSR.

When simulated 30,503 working face is at 100 m, the vertical stress distribution of each survey line within 4 m of the roadway floor at 0, 20, and 30 m ahead of the working face is shown in Figure 20. When mining the working face, the stress under the floor presents a “U-shaped” distribution. The stress value on the solid coal side is higher within the mining influence range, while the stress value on the coal pillar side is higher away from the mining influence. The overlying load is transmitted to the roadway floor through the two sides of the roadway, and the high vertical load on the floor is the direct cause for the continuous occurrence of the floor heave.

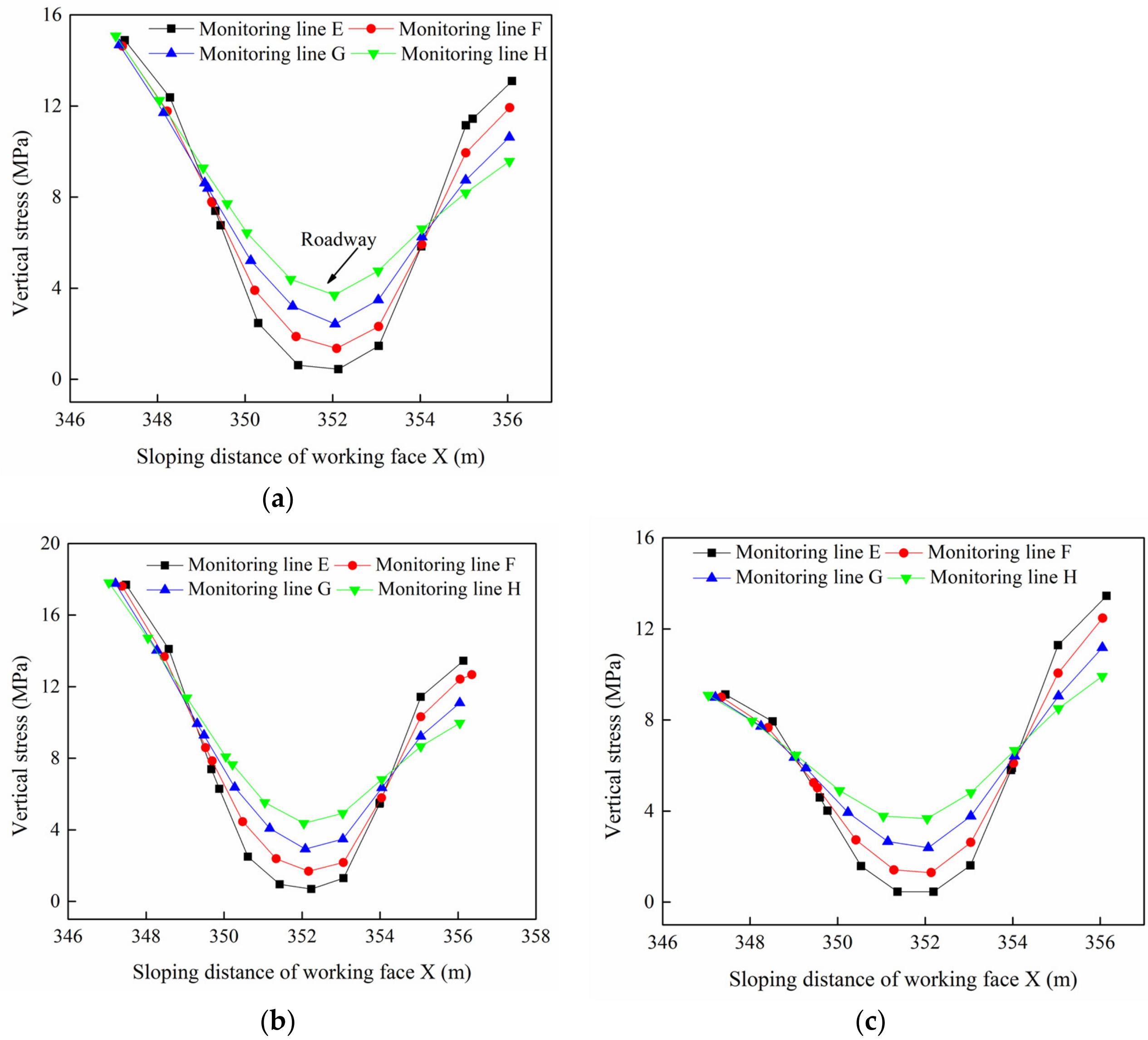

Figure 20. Vertical stress distribution at GSR floor. (**a**) 0 m ahead of the working face, (**b**) 20 m ahead of the working face [28], (**c**) 30 m ahead of the working face.

4.3.3. Displacement Distribution around the Roadway Affected by Mining

When 30,503 working face is at 100 m, the horizontal displacement changes along each survey line in the roadway sides within 30 m ahead of the working face is shown in Figure 21. The changing trend within 30 m is basically the same on two sides of the roadway. The maximum deformation on the solid coal side is 0.69 m, located at 1 m away from the sidewall. The deformation on the gob side increases continuously in coal pillar with a maximum displacement of 1.4 m. The deformations along the monitoring line B and C are larger than that along line D on the coal pillar side, which is basically consistent with the roadway deformation characteristics on site. Based on the above analysis, it can be concluded that the large deformation of the deep coal is an important cause for the occurrence of bulging on coal pillar side of the roadway. Also, there are only 2.2 m bolts for the coal pillar, which cannot control the heave effectively.

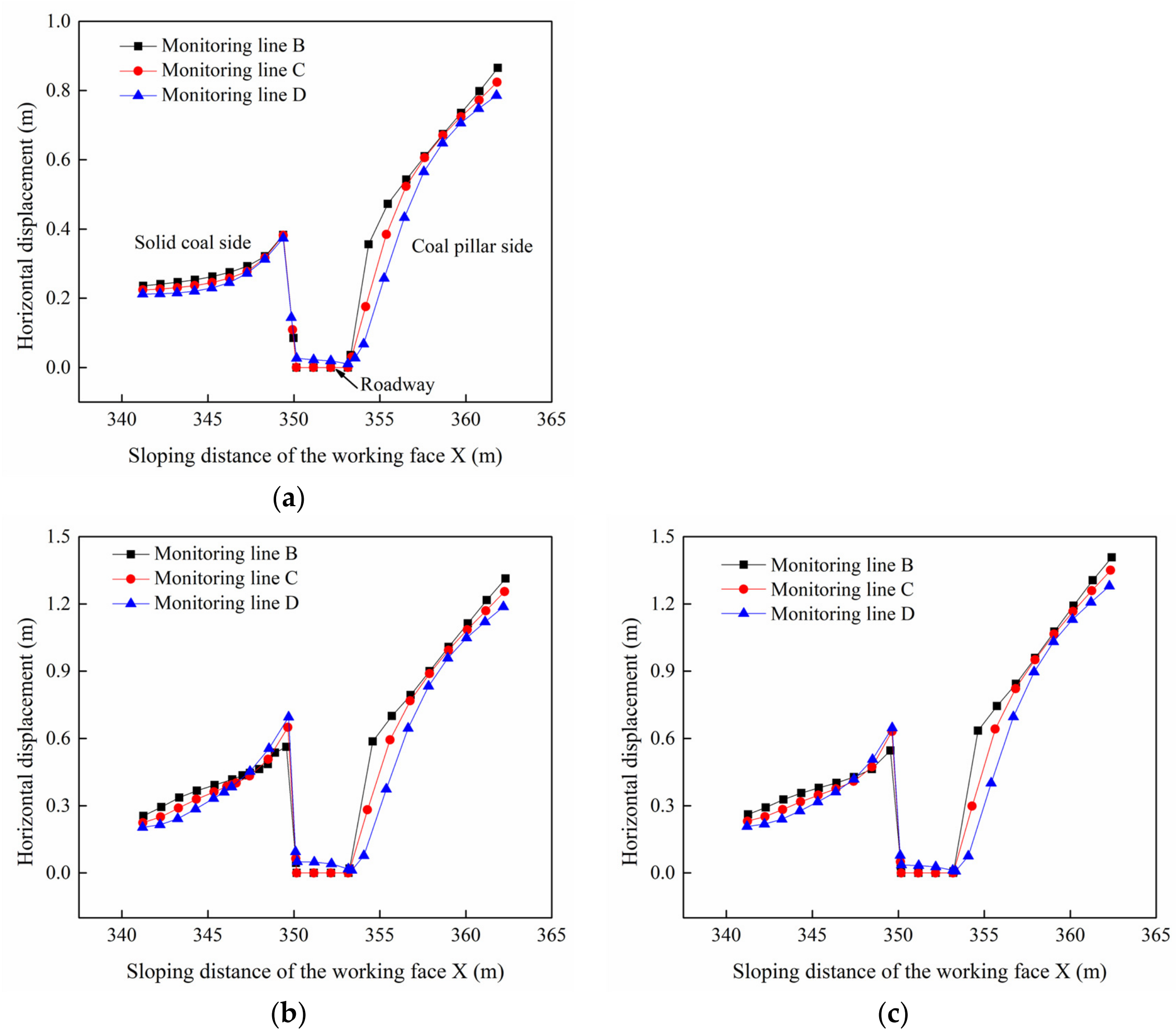

Figure 21. Horizontal displacement distribution of the roadway two sides. (**a**) 0 m ahead of the working face, (**b**) 20 m ahead of the working face [28], (**c**) 30 m ahead of the working face.

According to the research results obtained from the study. The middle part of roadway near the solid coal side, and the middle and upper of the roadway on coal pillar side within 20 m in front of the working face shall be strengthened on the basis of the existing support. Improving the rock bearing capacity on the coal pillar side and using longer bolts could be effective measures to ensure the stability of the GSR.

The vertical displacement changes in the roadway floor within 30 m ahead of the working face when 30,503 working face is at 100 m is shown in Figure 22. The maximum floor heave of 0.41 m appears in the middle roadway 20 m ahead of the working face. Due to high vertical stress in side walls, the roadway continues to heave, and the displacement gradually decreases with increasing distance from the floor. When it is 4 m away from the roadway floor, the displacement is basically negligible. Under the high unbalanced load, the floor is prone to heave plastically under the coupling action of the horizontal compression and the vertical stress. Meanwhile, the vertical stress generated by the breaking of the high and low old roofs acts on rocks surrounding the 30,503 GSR, and the load of overlying rocks is transmitted to the floor through the two sides of the roadway. Under the high stress, two corners of the floor displace downward, and hereby the roadway is squeezed and heave. When the high stress exceeds the ultimate strength of the floor, the floor will be squeezed out and fractured in the roadway.

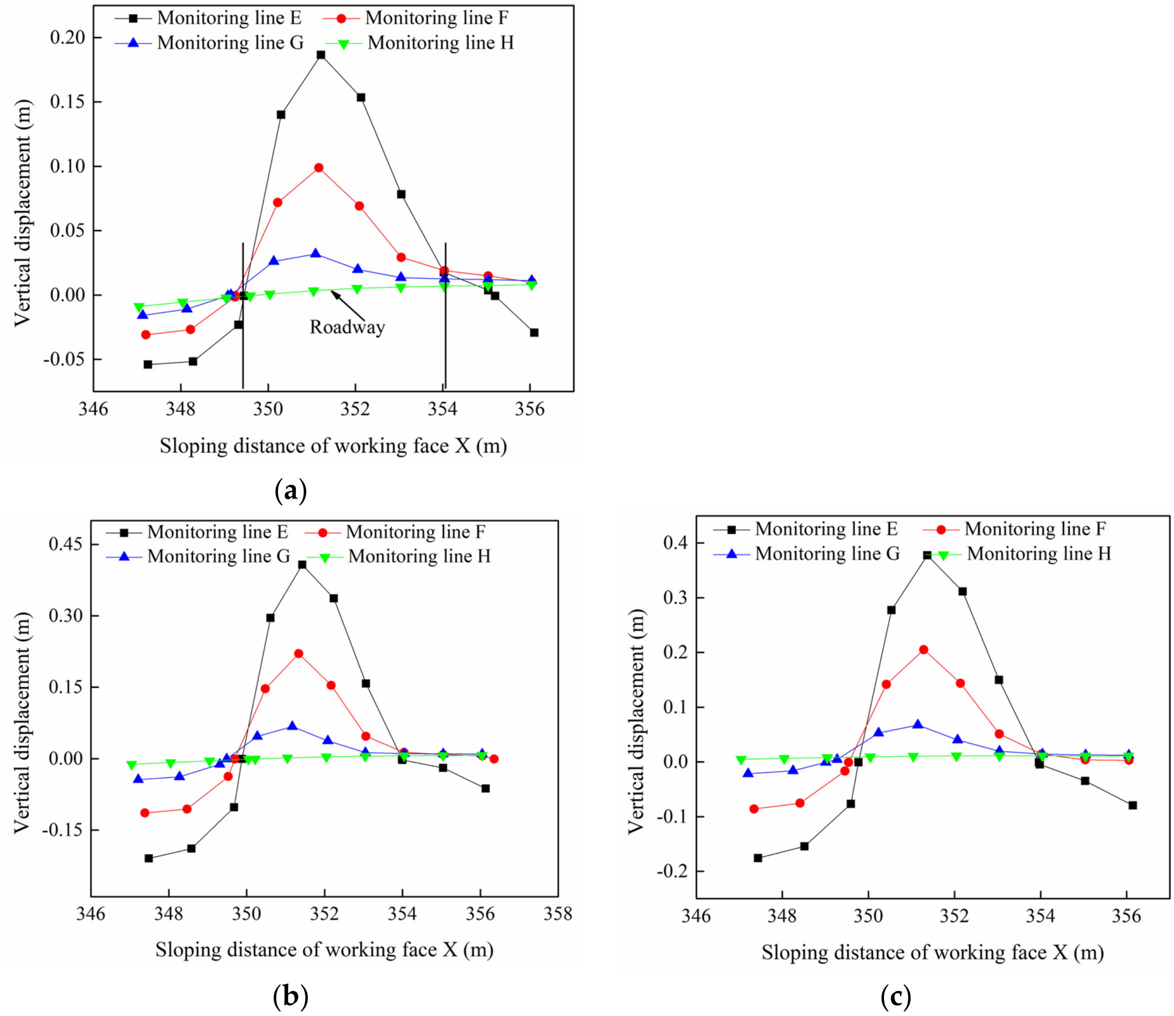

Figure 22. Vertical displacement distribution of the roadway floor. Two black line in (**a**) used to explain the location of roadway. (**a**) 0 m ahead of the working face, (**b**) 20 m ahead of the working face [28], (**c**) 30 m ahead of the working face.

5. Conclusions

(1) The fracturing and subsidence of the key layers accompanied by dense microseismic events have an important impact on the stress field surrounding the GSR. The deformation of the middle roadway on the solid coal side, the middle and upper roadway on the coal pillar side and the bottom of the roadway are relatively large.

(2) Under the influence of mining, the overlying strata of the GSR are broken to form a composite structure as "low-level cantilever beam and high-level masonry beam". The breaking and subsidence of the structures are the main cause for the stress and instability increase in the roadway. The breaking position of the low-level old roof is 1 m away from the coal pillar. The maximum transferred stress at the contact gangue point is 23.7 MPa.

(3) Shear and tension failure happen in the GSR due to overburden subsidence and rotary extrusion. The stress and displacement at the middle and upper coal pillar side of the roadway are relatively large. The peak stress in solid coal side is about 1.8 times that of the coal pillar side. The peak stress on the coal pillar side appears 2 m away from the roadway, which is close to the length of the bolt support. The maximum horizontal displacement on the coal pillar side is about 2 times that of the solid coal side.

(4) The mining-induced stress and the stress transferring at the gangue contact point are the direct reasons for side wall bulge on the the solid coal side. The peak stress in solid coal is 7 m away from the roadway, which is at the gangue contact point where overburden

breaks. The coupling effect of the overburden stress, the transferred stress near the gangue contact point, and the horizontal stress is the force source for the floor heave. The research results are of great significance to guide the targeted roadway support of similar mines.

Author Contributions: Writing original draft, S.H.; Conceptualization, S.H., L.G. and B.Z.; Methodology, S.H., L.G. and F.S.; Funding acquisition, S.H.; Validation, L.G. and T.C.; Investigation, B.Z., Z.L., X.H. and Y.M.; Formal analysis, X.H., Z.L., D.S. and F.S.; Supervision, X.H.; Writing—review &editing, Y.M. and D.S.; All authors have read and agreed to the published version of the manuscript.

Funding: This research was funded by the National Natural Science Foundation of China (No. 52204197), the Postdoctoral Research Foundation of China (Project No. 2021M700371), the Fundamental Research Funds for the Central Universities (Project No. FRF-TP-22-111A1), the Open fund of State Key Laboratory of Coal Mining and Clean Utilization (Project No. 2021-CMCU-KF013).

Institutional Review Board Statement: Not applicable.

Informed Consent Statement: Not applicable.

Data Availability Statement: Data can be obtained by contacting the corresponding author.

Conflicts of Interest: The authors confirm that there are no conflict of interest associated with this publication.

References

1. Han, C.L.; Yang, H.Q.; Zhang, N.; Deng, R.J.; Guo, Y.X. Zoning Control Technology of the gob-side roadway Driving with Small Coal Pillar Facing Mining in a Special Isolated Island Working Face: A Case Study. *Appl. Sci.* **2021**, *11*, 10744. [CrossRef]
2. Mu, H.W.; Wang, A.H.; Song, D.Z.; Su, D.F. Failure Mechanism of the gob-side roadway under Overlying Coal Pillar Multiseam Mining. *Shock. Vib.* **2021**, *2021*, 4403456. [CrossRef]
3. Chen, A. Width Design of Small Coal Pillar of Gob-Side Entry Driving in Soft Rock Working Face and Its Application of Zaoquan Coal Mine. *Adv. Civ. Eng.* **2021**, *2021*, 9999957. [CrossRef]
4. Yang, K.; Gou, P.F. Research on Reasonable Width of Coal Pillars in High Strength Mining Roadway in Wantugou Mine. *Geotech. Geol. Eng.* **2021**, *39*, 2065–2073. [CrossRef]
5. Wang, J.; Ning, J.G.; Tan, Y.L.; Hu, S.C.; Guo, W.Y. Deformation and failure laws of roadway surrounding rock and support optimization during shallow-buried multi-seam mining. *Geomat. Nat. Haz. Risk* **2020**, *11*, 191–211. [CrossRef]
6. Xu, X.H.; He, F.L.; Li, X.B.; He, W.R. Research on mechanism and control of asymmetric deformation of gob side coal roadway with fully mechanized caving mining. *Eng. Fail. Anal.* **2021**, *120*, 105097–105109. [CrossRef]
7. Liu, H.Y.; Zhang, B.Y.; Li, X.L.; Liu, C.W.; Wang, C.; Chen, D.Y. Research on roof damage mechanism and control technology of gob-side entry retaining under close distance gob. *Eng. Fail. Anal.* **2022**, *138*, 106331. [CrossRef]
8. He, F.L.; Xu, X.H.; Qin, B.B.; Li, L.; Lv, K.; Li, X.B. Study on deformation mechanism and control technology of surrounding rock during reuse of gob side entry retaining by roof pre-splitting. *Eng. Fail. Anal.* **2022**, *137*, 106271. [CrossRef]
9. Shi, J.J.; Feng, J.C.; Rui, P.; Zhu, Q.J. The research on stability of surrounding rock in gob-side entry driving in deep and thick seam. *Geotech. Geol. Eng.* **2022**, *40*, 3357–3364.
10. Xiong, X.Y.; Dai, J.; Ouyang, Y.B.; Shen, P. Experimental analysis of control technology and deformation failure mechanism of inclined coal seam roadway using non-contact DIC technique. *Sci. Rep.UK* **2021**, *11*, 20930–20954. [CrossRef] [PubMed]
11. Wang, Y.; Li, Y.M.; Yu, Z.L.; Zhang, H.; Ding, D. Research on the Surrounding Rock Control Technology of Gob-Side Entry with a Narrow Coal Pillar Reserved in a Fully Mechanized Caving Face with Large Mining Height. *Geotech. Geol. Eng.* **2021**, *40*, 285–300. [CrossRef]
12. Ma, Z.Q.; Chen, C.; Liang, X.C.; Chen, A.M.; Song, W.X. Field and numerical investigation on the stability of coal pillars of gob-side entry driving with top coal. *Arab. J. Geosci.* **2020**, *13*, 1193–1206. [CrossRef]
13. Gao, X.; Zhang, S.; Zi, Y.; Khan, S. Study on optimum layout of roadway in close coal seam. *Arab. J. Geosci.* **2020**, *13*, 746–759. [CrossRef]
14. Wang, X.F.; Lu, M.Y.; Gao, Y.H.; Luo, W.B.; Liu, W.G. Structural Mechanical Characteristics and Instability Law of Roof Key Block Breaking in the gob-side roadway. *Adv. Civ. Eng.* **2020**, *2020*, 6682303. [CrossRef]
15. Mo, S.; Sheffield, P.; Corbett, P.; Ramandi, H.L.; Oh, J.; Canbulat, L.; Saydam, S. A numerical investigation into floor buckling mechanisms in underground coal mine roadways. *Tunn. Undergr. Space Technol.* **2020**, *103*, 103497. [CrossRef]
16. Li, H.; Lin, B.Q.; Hong, Y.D.; Gao, Y.B.; Yang, W.; Liu, T.; Wang, R.; Huang, Z.B. Effects of in-situ stress on the stability of a roadway excavated through a coal seam. *Int. J. Min. Sci. Technol.* **2017**, *27*, 917–927. [CrossRef]
17. Zhao, Y.Q.; Li, X.B.; Hou, J.Q. Research on Asymmetric Failure Mechanism and Control Technology of Roadway Along Gob in Extra Thick Coal Seam. *Geotech. Geol. Eng.* **2021**, *40*, 1009–1021. [CrossRef]
18. Hua, X.Z.; Liu, X.; Huang, Z.G.; Yang, P.; Ma, Y. Stability mechanism of non-pillar gob-side entry retaining by roof cutting under the coupled static dynamic loading. *J. China Coal. Soc.* **2020**, *45*, 3696–3708.

19. Zhang, Y.; Xia, X.; Sun, X.M.; Song, P.; Wang, J.; Sun, S.J.; Chen, C. Research on Coupling Control Technology of Constant Resistance in Gob-side Entry Under Mined Gob of Recent Coal Seam Group. *Geotech. Geol. Eng.* **2020**, *38*, 4685–4699. [CrossRef]
20. Guo, P.F.; Zhang, X.H.; Peng, Y.Y.; He, M.C.; Ma, C.R.; Sun, D.J. Research on deformation characteristic and stability control of surrounding rock during gob-side entry retaining. *Geotech. Geol. Eng.* **2020**, *38*, 2887–2902. [CrossRef]
21. Zha, W.H.; Shi, H.; Liu, S.; Kang, C.H. Surrounding rock control of gob-side entry driving with narrow coal pillar and roadway side sealing technology in Yangliu Coal Mine. *Int. J. Min. Sci. Technol.* **2017**, *27*, 819–823. [CrossRef]
22. Zhou, X.M.; Wang, S.; Li, X.L. Research on theory and technology of floor heave control in semicoal rock roadway: Taking longhu coal mine in Qitaihe mining area as an Example. *Lithosphere* **2022**, *2022*, 3810988. [CrossRef]
23. Li, X.L.; Chen, S.J.; Wang, S. Study on in situ stress distribution law of the deep mine taking Linyi Mining area as an example. *Adv. Mater. Sci. Eng.* **2021**, *9*, 5594181. [CrossRef]
24. Li, G.; Ma, F.S.; Guo, J.; Zhao, H.J.; Liu, G. Study on deformation failure mechanism and support technology of deep soft rock roadway. *Eng. Geol.* **2020**, *264*, 105262–105276. [CrossRef]
25. Liu, D.J.; Zuo, J.P.; Wang, J.; Zhang, T.L.; Li, H.Y. Large deformation mechanism and concrete-filled steel tubular support control technology of soft rock roadway-A case study. *Eng. Fail. Anal.* **2020**, *116*, 104721. [CrossRef]
26. Zhang, W.; He, Z.M.; Zhang, D.S.; Qi, D.H.; Zhang, W.S. Surrounding rock deformation control of asymmetrical roadway in deep three-soft coal seam: A case study. *J. Geophys. Eng.* **2018**, *15*, 1917–1928. [CrossRef]
27. Xue, G.Z.; Gu, C.; Fang, X.Q.; Wei, T. A Case Study on Large Deformation Failure Mechanism and Control Techniques for Soft Rock Roadways in Tectonic Stress Areas. *Sustainability* **2019**, *11*, 3510. [CrossRef]
28. Zhao, B.; He, S.; He, X.; Gao, L.; Li, Z.; Song, D.; Shen, F. Research on Deformation and Failure Control Technology of a Gob-Side Roadway in Close Extra-Thick Coal Seams. *Sustainability* **2022**, *14*, 11246. [CrossRef]
29. Orlecka-Sikora, B. The role of static stress transfer in mining induced seismic events occurrence, a case study of the Rudna mine in the Legnica-Glogow Copper District in Poland. *Geophys. J. Int.* **2010**, *182*, 04672. [CrossRef]
30. Zhao, Y.Q. *Study on Narrow Time-Space Interval and Surrounding Rock Control of the Gob-Side Roadway for Fully-Mechanized Top Coal Caving Face in Extra-Thick Coal Seam*; China University of Mining and Technology: Beijing, China, 2019.
31. He, F.L.; Zhang, G.C. Deformation and failure mechanism and control technology of large section coal roadway subjected to severe mining dynamic load. *J. Min. Saf. Eng.* **2016**, *33*, 423–430.
32. Qu, X.K.; Jiang, F.X.; Wang, H.T.; Zhu, S.T.; Zhang, M.; Xu, K.; Zhang, W.T. Research on mechanism of rock burst induced by coal pillar failure in mine gob. *J. Min. Saf. Eng.* **2017**, *34*, 1134–1140.
33. Castelli, F.; Grasso, S.; Lentini, V.; Sammito, M.S.V. Effects of Soil-Foundation-Interaction on the Seismic Response of a Cooling Tower by 3D-FEM Analysis. *Geosciences* **2021**, *11*, 200. [CrossRef]

Disclaimer/Publisher's Note: The statements, opinions and data contained in all publications are solely those of the individual author(s) and contributor(s) and not of MDPI and/or the editor(s). MDPI and/or the editor(s) disclaim responsibility for any injury to people or property resulting from any ideas, methods, instructions or products referred to in the content.